



Synthetic talc as catalyst and filler for waterborne polyurethane-based nanocomposite synthesis

Guilherme Dias¹ · Manoela Prado¹ · Christophe Le Roux⁴ · Mathilde Poirier⁴ · Pierre Micoud⁴ · Rosane Ligabue^{1,2} · François Martin⁴ · Sandra Einloft^{1,3} 

Received: 17 January 2019 / Revised: 25 March 2019 / Accepted: 19 April 2019 / Published online: 23 April 2019
© Springer-Verlag GmbH Germany, part of Springer Nature 2019

Abstract

In this work, synthetic talc was used as catalyst and filler aiming to obtain waterborne polyurethane (WPU) nanocomposites by in situ polymerization. Filler was used both in gel and in powder forms in order to compare its effects into the WPU matrix. The use of synthetic talc as filler is interesting due to the possibility of hydrogen bond formation between WPU chains/Si–O–Si and OH groups in synthetic talc edges promoting changes in physical, mechanical and thermal properties. Moreover, WPUs are environmentally friendly polymers replacing organic solvents by water as dispersion medium reducing pollutant emission in the atmosphere. Material structure analyzed by FTIR evidenced that it is possible to synthesize WPU using synthetic talc as catalyst and proved hydrogen bonding formation between synthetic talcs and WPU matrix. Synthetic talcs were well dispersed even with higher filler content, as supported by XRD, TEM, FESEM and AFM analyses. Thermal and mechanical performance was improved with synthetic talc fillers' addition in order to obtain WPU nanocomposites. Also, T_g of WPU nanocomposites was affected by fillers' addition as presented by DSC corroborating synthetic talc good dispersion as evidenced by XRD and TEM analyses. Synthetic talcs used as catalyst/filler resulted in nanocomposites with superior thermal and mechanical properties being a new path to utilize synthetic talcs to obtain multifunctional materials.

Keywords Waterborne polyurethane · Synthetic talc · In situ polymerization · Hydrogen bond

Electronic supplementary material The online version of this article (<https://doi.org/10.1007/s00289-019-02789-w>) contains supplementary material, which is available to authorized users.

✉ Sandra Einloft
einloft@puers.br

Extended author information available on the last page of the article

Introduction

Waterborne polyurethane (WPU) is a polyurethane system in which water is used as dispersion medium replacing conventional organic solvents (toluene and acetone). The use of water as solvent reduces volatile organic compounds' (VOCs) release to the atmosphere contributing to environment protection [1]. WPU has interesting applications as adhesives, coatings and membranes owing to its good processing properties, abrasion resistance, non-toxicity, low cost and great adhesion [2, 3].

However, thermal stability, insolubility and mechanical properties of WPU are lower when compared to the organic solvent-borne PU which needs to be improved. Using nanoparticle fillers is an effective way to alter and enhance WPU properties [4]. In this context, various inorganic particles are used to obtain new nanocomposites, like Fe_3O_4 [1, 2, 5], silica [6–9], attapulgite [4], clay [10–13], metallic oxides [14–17], etc. Among all potential nanocomposite precursors, those based on clay and layered silicates have been most widely investigated, probably due to the easy availability of starting clay materials. Moreover, talc particles are widely used as plate-like mineral filler because it is a low-cost material [18]. Despite their good performance as filler and low price, natural talc presents some drawbacks. Natural talc cannot be ground homogeneously below $5\ \mu\text{m}$ without leading to structure amorphization. To solve this issue and also to control particle size, we turned to talc obtained from hydrothermal synthesis [19]. Synthetic talcs used as fillers were reported by many researches to produce new materials such as solvent-borne polyurethanes [20–24], polypropylene and polyamide 6 (PA6) nanocomposites [18], PP/PA6 blends [25], PP/PA6 blends using ionic liquids/nanotalc as fillers [26], PA6 and PA12 nanocomposites [27], ternary nanotalc reinforced PA6/SEBS-g-MA composites [28] and also WPUs [29, 30]. Moreover, tin catalysts as dibutyl tin dilaurate (DBTDL), widely used as catalyst in PU synthesis, are known as toxic compounds [31]; for this reason, it is interesting to use environmentally friendly catalysts, like synthetic talc. As far as we know in this work, we describe for the first time the use of synthetic talc as catalyst. Filler effect in polymerization reaction as catalyst and as reinforcement in waterborne polyurethane nanocomposite properties was evaluated as well.

Experimental

Materials

Synthetic talcs were manufactured using the following materials: magnesium acetate tetrahydrate ($\text{Mg}(\text{CH}_3\text{COO})_2 \cdot 4\text{H}_2\text{O}$), sodium metasilicate pentahydrate ($\text{Na}_2\text{SiO}_3 \cdot 5\text{H}_2\text{O}$), sodium acetate trihydrate ($\text{NaCH}_3\text{COO} \cdot 3\text{H}_2\text{O}$) and acetic acid. All reagents were purchased from Sigma-Aldrich and used without further purification.

Isophorone diisocyanate (IPDI, for synthesis, Bayer, Germany), polyester diol ($M_n = 1000\ \text{g/mol}$) and 2,2-bis(hydromethyl) propionic acid (DMPA, 99%,

Perstorp, Sweden) were used to obtain waterborne polyurethanes. NCO/OH molar ratio of 1:7 was utilized. Dibutyl tin dilaurate [DBTDL Miracema Nuodex Ind., Brazil (0.1% w/w)] was used as catalyst for pristine WPU. DMPA carboxylic acid was neutralized with trimethylamine (J.T Baker, Center Valley, Pennsylvania, USA). Free NCO content was measured by titration with *n*-dibutylamine (Bayer, Leverkusen, Germany), and hydrazine (Merck, Kenilworth, NJ, USA) was used as chain extender.

Synthetic talc preparation

Synthetic talc was obtained by hydrothermal synthesis as described in the literature [32]. First, talc precursor was obtained by reacting sodium metasilicate pentahydrate with magnesium acetate tetrahydrate in a proportion of Si/Mg=4/3, in the presence of sodium acetate. In a second step, talc precursor was hydrothermally treated under high temperature (300 °C) and pressure (85 bar) during a period of time of 6 h in order to obtain well-crystallized nano-sized talc gel. Synthetic talc (ST) was obtained in gel form (ST-g) or in powder form (ST-p) after drying in an oven at 120 °C and grinding. Specific surface area of synthetic talc manufactured in these conditions is 130 m² g⁻¹, as reported previously by our group [29].

Waterborne polyurethane nanocomposite preparation method

Waterborne polyurethane nanocomposites and pristine waterborne polyurethane were prepared by in situ polymerization. In a glass reactor, the following reagents were placed: IPDI, the polyester diol and DMPA (NCO/OH molar ratio of 1:7 and 5% w/w of DMPA in relation to prepolymer solid content). The NCO-terminated prepolymer reaction was carried out under constant mechanical stirring and inert atmosphere (N₂) at 80 °C for 1 h. To quantify the residual-free isocyanate content, titrations were performed with *n*-dibutylamine based on the ASTM 2572 standard technique. Then, to neutralize the acid groups from DMPA, molar equivalent of trimethylamine was added to the reactor and stirred for 30 min at 50 °C as previously described in the literature [16, 29]. Lastly, a mixture of the previously neutralized prepolymer and hydrazine (chain extender in amount equivalent to the residual-free NCO content) was poured in water and kept under mild agitation (200 rpm) at room temperature for 30 min. To prepare pristine WPU, DBTDL was used as catalyst. To produce WPU nanocomposites, synthetic talc in gel and powder form was used aiming to substitute DBTDL as catalyst and perform as reinforcement. Filler content was 0.5 wt%, 1 wt% and 3 wt%. The average solid content was 37% w/w. Lastly, films with 70 µm of thickness were produced by casting.

Characterization methods

Fourier transform infrared spectroscopy (FTIR)

The films were characterized by Fourier transform infrared spectroscopy (FTIR, PerkinElmer Spectrum 100 spectrometer) in transmission mode in the range 4000–650 cm^{-1} , to ascertain filler and nanocomposite structural properties.

X-ray diffraction analysis (XRD)

X-ray diffraction (Shimadzu XRD-7000) patterns were recorded with $\text{CuK}\alpha_{1,2}$ Bragg–Brentano geometry θ – θ radiations, between 5° and 80° with a step size of 0.028, voltage of 40 kV and current of 30 mA.

Differential scanning calorimetry (DSC)

Differential scanning calorimetry (DSC, TA Instruments Q20 calorimeter) was used to determine glass transition temperature (T_g) from –90 to 200 °C, with a heating rate of 10 °C/min under an inert atmosphere of nitrogen, from the second heat cycle.

Thermogravimetric analysis (TGA)

Thermogravimetric analysis (TA Instruments Q600 simultaneous thermal analyzer) was carried out with a heating rate of 20 °C/min, from room temperature to 800 °C under nitrogen atmosphere.

Tensile strength analysis

Mechanical tests were performed in triplicate according to ASTM D822 standard technique (TA Instruments Q800 dynamic mechanical analyzer) for determination of Young's modulus and stress \times strain tests.

Field emission scanning electron microscopy (FESEM)

Field emission scanning electron microscopy (FESEM, FEI Inspect F50) analyses were performed in secondary electron (SE) mode and used for the assessment of filler distribution in the polymer matrix.

Atomic force microscopy (AFM)

Atomic force microscopy (AFM) was used to collect roughness data of the WPU and its nanocomposites. The AFM analyses were performed in tapping mode to construct phase/height contrast images at different locations on the top surface of the samples using a Bruker Dimension Icon PT equipped with a TAP150A probe

(resonance frequency of 150 kHz and 5 N m^{-1} spring constant) and calibrated prior to sample measurements. The scanned area of images was $5 \times 5 \mu\text{m}^2$ with a resolution of 512 frames per area.

Results and discussion

FTIR analysis

WPU nanocomposites, neat WPU, synthetic talc in gel and in powder form were characterized by FTIR spectroscopy (Fig. 1). In synthetic talc spectra (ST-p and

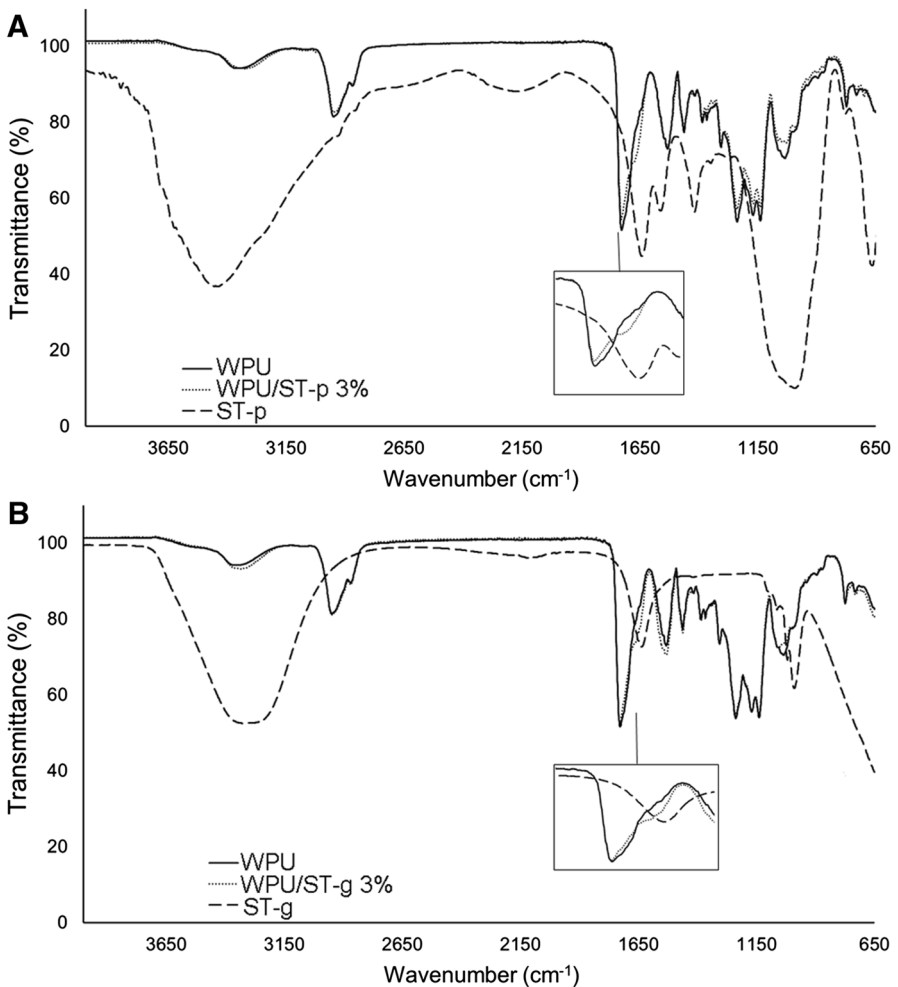


Fig. 1 FTIR spectra of **A** neat WPU, WPU/ST-p 3% and ST-p and **B** neat WPU, WPU/ST-g 3% and ST-g

ST-g), it was observed characteristic bands assigned to talc around 1650 cm^{-1} related to Si–O vibrations [33] and the band between 1200 and 800 cm^{-1} characteristic of Si–O and Si–O–Si bonds [20, 23, 24, 33, 34]. For neat WPU and its nanocomposites, the bands in regions of 3500 – 3400 cm^{-1} are attributed to urethane linkage N–H. The bands in 2950 and 2870 cm^{-1} are associated with different vibrational modes of polymeric chain CH_2 group. The band in 1731 cm^{-1} is characteristic of C=O of urethane bond. Region around 1520 cm^{-1} is related to CN and NH of urethane bonds. CO–O bond appears in 1243 cm^{-1} region. In 1185 and 1135 cm^{-1} appear the bands associated with N–CO–O and C–O–C groups [13, 15, 20–24, 29, 30]. WPU nanocomposite formation is proved by FTIR (Fig. 1), confirming synthetic talc as a substitute for commercial catalyst in polymerization reaction. It also can be observed that the band related with C=O decreases as filler content increased and a shoulder appeared around 1650 cm^{-1} in the nanocomposites, probably due to hydrogen bond formation between C=O of polymeric chain and hydroxyl groups available on synthetic talc layer edges [16].

XRD-TEM analysis

Figure 2A, C shows diffraction patterns of pristine WPU, synthetic talcs and their nanocomposites. Characteristic XRD diffraction peaks associated with natural talc are observed, but for synthetic talcs these diffraction peaks are broader and less intense. This behavior indicates that synthetic talc layers are smaller compared

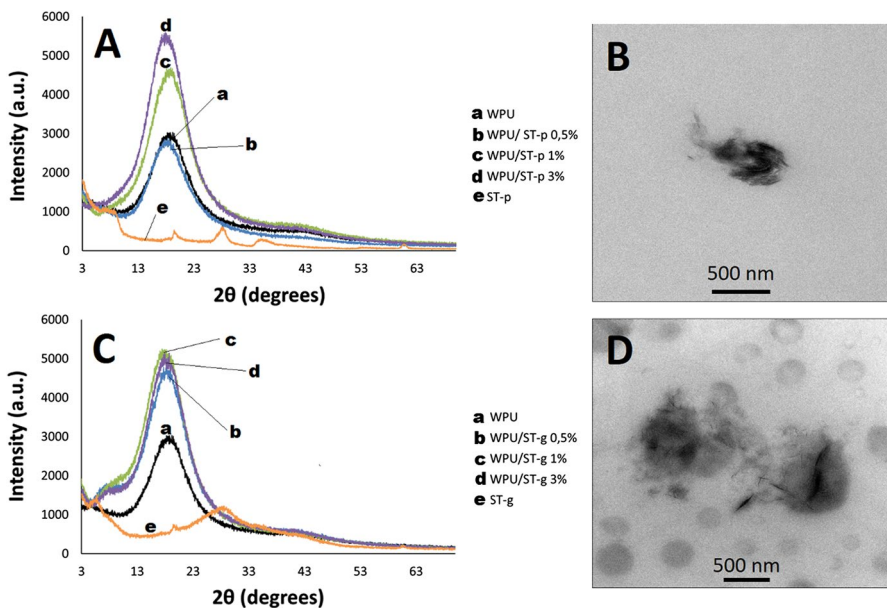


Fig. 2 XRD patterns of **A** WPU/ST-p and **C** WPU/ST-g nanocomposites, compared to neat WPU and synthetic talc. TEM images of **B** WPU/ST-p 3% and **D** WPU/ST-g 3%

to natural talc [18, 19, 22, 29]. For pure WPU films, a broad diffraction peak is located around $2\theta=20^\circ$; this diffraction is associated with PU amorphous phase and appeared in all nanocomposite samples [2]. The diffraction peak around $2\theta\cong 9^\circ$ for synthetic talc in powder form disappeared in WPU/ST-p nanocomposite XRD pattern, suggesting that polymer enters between two nanoparticle layers leading to the layer intercalation and resulting in good filler dispersion throughout WPU films [3]. Characteristic diffraction peaks of synthetic talc in gel form appeared in WPU/ST-g nanocomposite diffraction patterns. Moreover, this peak located at $2\theta\cong 9^\circ$ raised in XRD patterns of WPU nanocomposites with ST-g content, indicating that synthetic talc in gel form layers is intercalated between two individual nanoparticles [35, 36]. Figure 2B, D shows TEM images of WPU/ST nanocomposite samples containing 3 wt% of synthetic talc. As illustrated in TEM images, the dark areas are attributed to ST fillers and lighter colored region attributed to WPU matrix [2]. With 3 wt% of filler content into the WPU matrix, we observed that for sample ST-p 3% a good dispersion was not achieved although a degree of dispersion is observed in ST-g 3% sample, see Fig. 2B, D [20, 22, 23, 25, 28, 30].

Mechanical properties

Table 1 presents stress/strain properties of neat WPU and WPU nanocomposites. Synthetic talc addition affected nanocomposite mechanical properties. The nanocomposites do not break at test conditions. Interactions between filler and polymer alternatively to filler and filler interactions are probably associated with mechanical properties enhancement [21–23, 29]. Well-dispersed fillers in polymer matrix as well as strong interfacial interaction between polymer and filler improved the stress transfer between polyurethane matrix and fillers increasing polymer resistance to deformation. This augmentation in mechanical properties can be related to hydrogen bonding between synthetic talcs and WPU in nanocomposites [37]. Young's modulus tended to increase with increasing filler content into the WPU nanocomposites; sample with 1 wt% of synthetic talc in gel form presented a different behavior, probably because some agglomeration occurred and affected WPU film formation and its mechanical performance. Moreover, talcs with high aspect ratio tend to stiffen materials [38]. Yet, this stiffening may be related to hydrogen bonding interactions, corroborating FTIR results [29, 39]. Our group showed in the previous works that

Table 1 Mechanical properties of the nanocomposites and neat WPU

| Samples | Young's modulus (MPa) | Strain (%) | Stress (MPa) |
|---------------|-----------------------|--------------|---------------|
| WPU | 31 ± 3 | 136 ± 9 | 6 ± 0.6 |
| WPU/ST-p 0.5% | 80 ± 9 | 97 ± 13 | 11 ± 1 |
| WPU/ST-p 1% | 38 ± 4 | 137 ± 12 | 7 ± 2 |
| WPU/ST-p 3% | 64 ± 12 | 115 ± 21 | 10 ± 2 |
| WPU/ST-g 0.5% | 35 ± 10 | 93 ± 30 | 6.5 ± 0.6 |
| WPU/ST-g 1% | 108 ± 1 | 4 ± 1 | 4 ± 0.8 |
| WPU/ST-g 3% | 49 ± 4 | 77 ± 39 | 8 ± 1 |

synthetic talc filler improved Young's modulus of WPU nanocomposites, like for WPU/synthetic talc nanocomposites formed by blending method [29] and WPU/ Fe_3O_4 synthetic talc nanocomposites also by blending method [30]. These results corroborate with TEM results and reinforce the fact that dispersion affects nanocomposite mechanical properties.

Thermal properties

In order to investigate thermal stability of neat WPU, WPU nanocomposites and the effect of the synthetic talcs on their thermal behavior, TGA was carried out (Figure S1). Results are listed in Table 2. It was observed from TGA data that WPU film thermal stability was enhanced by fillers' addition, which can be attributed to the action of nanoparticles as thermal insulator. Also the good filler dispersion into the WPU matrix resulted in an improvement in thermal stability of nanocomposite films [2]. The first stage is related to hard segment degradation and the second stage to soft segment degradation. Layered silicates can make the path longer for thermally decomposed volatiles to escape. It is clearly observed that the initial stage thermal decomposition temperature is the major and sharp which involves the thermal decomposition of the intercalated polymers [13]. The increase in the decomposition temperature is likely due to the interaction between WPU and fillers. Synthetic talc structure into the WPU matrix could limit the segmental movement of polymer chains or act as thermal insulator and mass transport barrier to the volatile products generated during decomposition, as a consequence retarding material degradation [8, 14]. In the previous works, it was reported that the thermal stability of nanocomposites is improved by the use of synthetic talc, because the large amount of hydroxyl groups present at the filler layer edges favors interactions between filler and polymer [21–23, 40]. But when nanocomposites with synthetic talc in gel form were prepared by physical mixture, thermal stability did not increase as when nanocomposites prepared by in situ polymerization, as reported in a previous work [29].

Thermal property of neat WPU and WPU nanocomposite films was studied by DSC (Figure S2). No melting peak was found in the DSC analysis for the pristine WPU and WPU/synthetic talc samples, indicating that no crystallization domain was formed in their hard or soft phases. This is corroborated with XRD results that

Table 2 Thermal properties of the nanocomposites and neat WPU

| Samples | T_{onset} (°C) | T_{peakmax1} (°C) | T_{peakmax2} (°C) | $T_{\text{g-DSC}}$ (°C) |
|---------------|-------------------------|----------------------------|----------------------------|-------------------------|
| WPU | 330.2 | 373.2 | 430.6 | – 33.3 |
| WPU/St-p 0.5% | 341.7 | 367.1 | 435.2 | – 34.9 |
| WPU/ST-p 1% | 348.3 | 376.9 | 439.7 | – 33.5 |
| WPU/ST-p 3% | 336.9 | 358.8 | 431.4 | – 37.1 |
| WPU/St-g 0.5% | 344.8 | 372.4 | 440.6 | – 37.2 |
| WPU/ST-g 1% | 338.4 | 369.4 | 431.9 | – 40.1 |
| WPU/ST-g 3% | 338.2 | 364.1 | 435.9 | – 40.6 |

show these polymers are amorphous [12]. Higher concentration of synthetic talc slightly decreased T_g . This effect could be associated with filler dispersion, as shown by XRD, TEM and FESEM results [41]. Also, phase separation could increase due to breakage of H-bonds between hard and soft segments decreasing T_g values [2, 17].

Morphological study

FESEM was employed to inspect nanocomposite microstructure. FESEM images of samples' fractured section are illustrated in Fig. 3. Figure 3 shows FESEM micrographs of neat WPU and WPU nanocomposites. All samples showed deeper and longer cracks when fractured with liquid nitrogen comparing with neat WPU. However, with the increasing filler content fracture surfaces became rough. This is related to the alteration of WPU matrix after adding higher filler content. This trend could be explained by supposing a homogenous nanoparticle distribution and an improvement in polymer/filler interaction in the nanocomposites, and therefore, a crack propagation path occurs inside the polyurethane matrix [8]. The rough fracture surface indicates that there was a strong resistance to further crack propagation. Meanwhile, the rough fracture surface means that a large crack would encounter difficulties in propagating. This effect can be responsible for nanocomposite mechanical properties improvement [42].

AFM results

Figure 4 shows the height AFM topographic images, and Table 3 shows the average roughness (R_a), root mean square roughness (R_q) and maximum height roughness (R_{max}) for neat WPU and its nanocomposites measured by AFM in

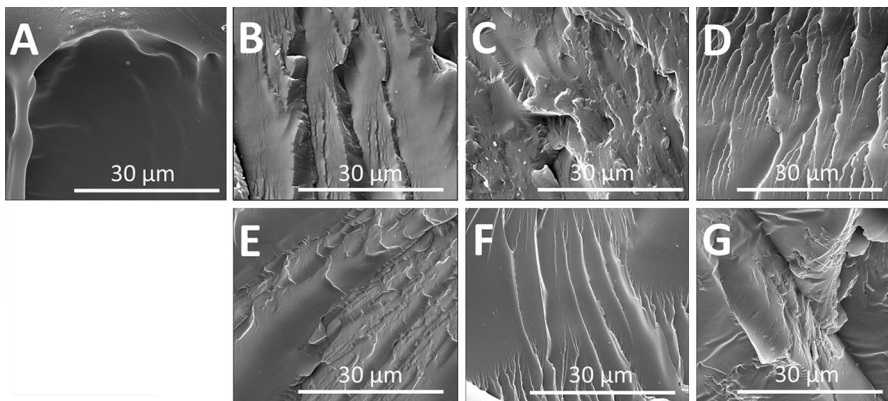


Fig. 3 Micrographs from cryogenically fractures of the materials at magnification of $\times 5000$, mode SE, **A** WPU, **B** WPU/St-p 0.5%, **C** WPU/ST-p 1%, **D** WPU/ST-p 3%, **E** WPU/St-g 0.5%, **F** WPU/ST-g 1% and **G** WPU/ST-g 3%

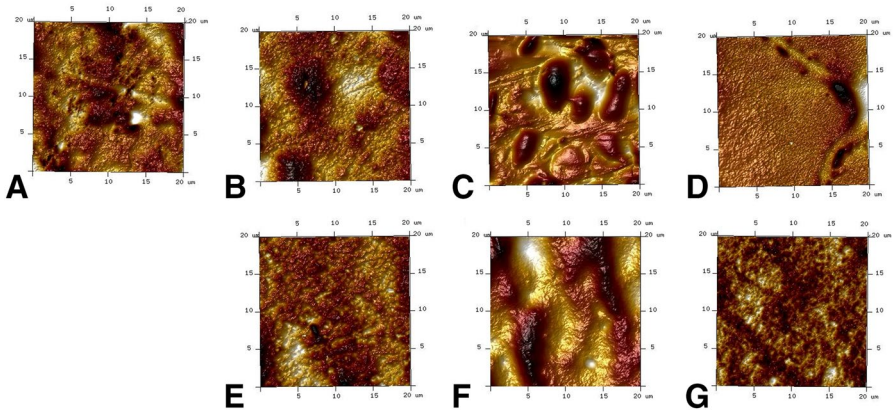


Fig. 4 AFM images (height). **A** WPU, **B** WPU/St-p 0.5%, **C** WPU/St-p 1%, **D** WPU/St-p 3%, **E** WPU/St-g 0.5%, **F** WPU/St-g 1% and **G** WPU/St-g 3%

Table 3 AFM results: average roughness (R_a), root mean square roughness (R_q), and maximum height roughness (R_{max}) of neat WPU and its nanocomposites

| Samples | R_q (nm) | R_a (nm) | R_{max} (nm) |
|---------------|------------|------------|----------------|
| WPU | 9 | 7 | 116 |
| WPU/St-p 0.5% | 59 | 46 | 431 |
| WPU/St-p 1% | 78 | 58 | 585 |
| WPU/St-p 3% | 24 | 13 | 330 |
| WPU/St-g 0.5% | 55 | 49 | 362 |
| WPU/St-g 1% | 142 | 115 | 805 |
| WPU/St-g 3% | 20 | 16 | 148 |

tapping mode. In WPU matrix (Fig. 4A), dark regions are associated with amorphous domains (soft segments) and bright regions are associated with crystalline domains (hard segments). The results of R_a , R_q and R_{max} demonstrate that with fillers' addition surface roughness of nanocomposites increased, indicating fillers' influence on the surface morphology of systems [29, 43]. As shown in Fig. 4, with fillers' addition on nanocomposites the rugged domains come more prominent evidencing the interactions between filler and polymer probably by hydrogen bonding among fillers and hard segments of the WPU [9, 29]. It can be seen that when 3 wt% of fillers was added to the WPU matrix, roughness decreased. Introducing higher filler content into WPU matrix restricted the shrinkage of the polymer surface, reducing nanocomposite roughness [10]. The higher values of these parameters comparing to pristine WPU confirm the presence of filler particles on the surface, as reported in the literature [11]. This interaction corroborates the mechanical properties improvements in nanocomposites once compared to pristine WPU.

Conclusions

New waterborne polyurethane nanocomposites were synthesized using synthetic talcs as catalyst and as filler by in situ polymerization. FTIR confirmed that it is possible to produce WPU/synthetic talc nanocomposites without adding the commercial catalyst. Also, FTIR indicated hydrogen bonds between filler and polymer chains. Synthetic talcs were well dispersed into the WPU matrix as supported by XRD, TEM, FESEM and AFM analyses. Thermal stability of WPU nanocomposites increased when compared to pristine WPU. DSC indicated that the glass transition temperature of nanocomposites was affected by the addition of synthetic talcs, probably due to good filler dispersion. Mechanical properties improvement can be associated with hydrogen bonding between filler and polymer and good filler dispersion. It has been proved that synthetic talc can be used as catalyst and filler to produce WPU nanocomposites with desired properties. This new waterborne polyurethane synthetic talc nanocomposites can be used for flexible films and/or coating industries.

Acknowledgements GD and MP thank CAPES for their PhD scholarship. SE acknowledges CNPq for DT Grant (Number 303467/2015-0). This study was financed in part by the Coordenação de Aperfeiçoamento de Pessoal de Nível Superior—Brasil (CAPES)—Finance Code 001. Thanks to Nokxeller—Microdispersions by the supply of part of the reagents used in this work.

References

1. Chen S, Zhang S, Jin T, Zhao G (2016) Synthesis and characterization of novel covalently linked waterborne polyurethane/Fe₃O₄ nanocomposite films with superior magnetic, conductive properties and high latex storage stability. *Chem Eng J* 286:249–258
2. Hoseini Z, Nikje MMA (2018) Synthesis and characterization of a novel thermally stable water dispersible polyurethane and its magnetic nanocomposites. *Iran Polym J* 27:733. <https://doi.org/10.1007/s13726-018-0650-5>
3. Gurunathan T, Mohanty S, Nayak SK (2015) Effect of reactive organoclay on physicochemical properties of vegetable oil-based waterborne polyurethane nanocomposites. *RSC Adv* 5:11524
4. Peng L, Zhou L, Li Y, Pan F, Zhang S (2011) Synthesis and properties of waterborne polyurethane/attapulgite nanocomposites. *Compos Sci Technol* 71:1280–1285
5. Zhang S, Li Y, Peng L, Li Q, Chen S, Hou K (2013) Synthesis and characterization of novel waterborne polyurethane nanocomposites with magnetic and electrical properties. *Compos Part A Appl Sci Manuf* 55:94–101. <https://doi.org/10.1016/j.compositesa.2013.05.018>
6. Chen JJ, Zhu CF, Deng HT et al (2009) Preparation and characterization of the waterborne polyurethane modified with nanosilica. *J Polym Res* 16:375. <https://doi.org/10.1007/s10965-008-9238-7>
7. Zhang SW, Liu R, Jiang JQ, Yang C, Chen M, Liu XY (2011) Facile synthesis of waterborne UV-curable polyurethane/silica nanocomposites and morphology, physical properties of its nanostructured films. *Prog Org Coat* 70:1–8
8. Peruzzo PJ, Anbinder PS, Pardini FM, Pardini OR, Plivelic TS, Amalvy JI (2016) On the strategies for incorporating nanosilica aqueous dispersion in the synthesis of waterborne polyurethane/silica nanocomposites: effects on morphology and properties. *Mater Today Commun* 6:81–91
9. Han Y, Chen Z, Dong W, Xin Z (2015) Improved water resistance, thermal stability, and mechanical properties of waterborne polyurethane nanohybrids reinforced by fumed silica via in situ polymerization. *High Perform Polym* 27:824–832
10. Kuan H, Ma CM, Chuang W, Su H (2005) Hydrogen bonding, mechanical properties, and surface morphology of clay/waterborne polyurethane nanocomposites. *J Polym Sci B Polym Phys* 43:1–12. <https://doi.org/10.1002/polb.20256>

11. Maji PK, Bhowmick AK (2012) Efficacy of clay content and microstructure of curing agents on the structure–property relationship of new-generation polyurethane nanocomposites. *Polym Adv Technol* 23:1311–1320
12. Rafiemanzelat F, Adli V, Mallakpour S (2015) Effective preparation of clay/waterborne Azo-containing polyurethane nanocomposite dispersions incorporated anionic groups in the chain termini. *Des Mono Polym* 18:303–314. <https://doi.org/10.1080/15685551.2014.999459>
13. Ramesh S, Punithamurthy K (2017) The effect of organoclay on thermal and mechanical behaviors of thermoplastic polyurethane nanocomposites. *Dig J Nanomater Biostruct* 12:331–338
14. Gao X, Zhu Y, Zhou S, Gao W, Wang Z, Zhou B (2011) Preparation and characterization of well-dispersed waterborne polyurethane/CaCO₃ nanocomposites. *Coll Surf A Physicochem Eng Asp* 377:312–317. <https://doi.org/10.1016/j.colsurfa.2011.01.025>
15. Demétrio da Silva V, dos Santos LM, Subda SM et al (2013) Synthesis and characterization of polyurethane/titanium dioxide nanocomposites obtained by in situ polymerization. *Polym Bull* 70:1819. <https://doi.org/10.1007/s00289-013-0927-y>
16. Soares RR, Carone C, Einloft S et al (2014) Synthesis and characterization of waterborne polyurethane/ZnO composites. *Polym Bull* 71:829. <https://doi.org/10.1007/s00289-014-1095-4>
17. Malik M, Kaur R (2018) Mechanical and thermal properties of castor oil-based polyurethane adhesive: effect of TiO₂ filler. *Adv Polym Technol* 37:24–30. <https://doi.org/10.1002/adv.21637>
18. Yousfi M, Livi S, Dumas A, Le Roux C, Crépin-Leblond J, Greenhill-Hooper M, Duchet-Rumeau J (2013) Use of new synthetic talc as reinforcing nanofillers for polypropylene and polyamide 6 systems: thermal and mechanical properties. *J Coll Interface Sci* 403:29–42
19. Dumas A, Martin F, Ferrage E, Micoud P, Le Roux C, Petit S (2013) Synthetic talc advances: coming closer to nature, added value, and industrial requirements. *Appl Clay Sci* 85:8–18
20. Dias G, Prado MA, Carone C et al (2015) Synthetic silico-metallic mineral particles (SSMMP) as nanofillers: comparing the effect of different hydrothermal treatments on the PU/SSMMP nanocomposites properties. *Polym Bull* 72:2991. <https://doi.org/10.1007/s00289-015-1449-6>
21. Prado MA, Dias G, Carone C, Ligabue R, Dumas A, Roux C, Micoud P, Martin F, Einloft S (2015) Synthetic Ni-talc as filler for producing polyurethane nanocomposites. *J Appl Polym Sci* 132:41854. <https://doi.org/10.1002/app.41854>
22. dos Santos LM, Ligabue R, Dumas A, Le Roux C, Micoud P, Meunier JF, Martin F, Einloft S (2015) New magnetic nanocomposites: polyurethane/Fe₃O₄-synthetic talc. *Eur Polym J* 69:38–49
23. Dias G, Prado M, Ligabue R, Poirier M, Le Roux C, Martin F, Fery-Forgues S, Einloft S (2018) Synthetic talc as a new platform for producing fluorescent clay polyurethane nanocomposites. *Appl Clay Sci* 158:37–45
24. Dias G, Prado M, Ligabue R, Poirier M, Le Roux C, Micoud P, Martin F, Einloft S (2018) Hybrid Pu/synthetic talc/organic clay ternary nanocomposites: thermal, mechanical and morphological properties. *Polym Polym Compos* 26:127–140
25. Yousfi M, Livi S, Dumas A, Crépin-Leblond J, Greenhill-Hooper M, Duchet-Rumeau J (2014) Compatibilization of polypropylene/polyamide 6 blends using new synthetic nanosized talc fillers: morphology, thermal, and mechanical properties. *J Appl Polym Sci* 131:40453. <https://doi.org/10.1002/app.40453>
26. Yousfi M, Livi S, Dumas A, Crépin-Leblond J, Greenhill-Hooper M, Duchet-Rumeau J (2015) Ionic compatibilization of polypropylene/polyamide 6 blends using an ionic liquids/nanotalc filler combination: morphology, thermal and mechanical properties. *RSC Adv* 5:46197. <https://doi.org/10.1039/c5ra00816f>
27. Beuguel Q, Ville J, Crepin-Leblond J, Mederic P, Aubry T (2015) Comparative study of the structural and rheological properties of PA6 and PA12 based synthetic talc nanocomposites. *Polymer* 62:109–117. <https://doi.org/10.1016/j.polymer.2015.02.031>
28. Hemlata MSN (2014) Mechanical, morphological, and thermal properties of nanotalc reinforced PA6/SEBS-g-MA composites. *J Appl Polym Sci* 132:41381. <https://doi.org/10.1002/app.41381>
29. Dias G, Prado M, Le Roux C, Poirier M, Micoud P, Ligabue R, Martin F, Einloft S (2017) Analyzing the influence of different synthetic talcs in waterborne polyurethane nanocomposites obtainment. *J Appl Polym Sci* 135:46107. <https://doi.org/10.1002/app.46107>
30. dos Santos LM, Ligabue R, Dumas A et al (2018) Waterborne polyurethane/Fe₃O₄-synthetic talc composites: synthesis, characterization, and magnetic properties. *Polym Bull* 75:1915. <https://doi.org/10.1007/s00289-017-2133-9>

31. Fernandes IP, Costa MRPFN, Ferreira MJ, Barreiro MF (2015) Water-based poly(urethane-urea) dispersions—meeting the European Union legislation. *Polymery* 60:536–540. <https://doi.org/10.14314/polimery.2015.536>
32. Le Roux C, Martin F, Micoud P, Dumas A (2013) Process for preparing a composition comprising synthetic mineral particles and composition. *Int. Pat. WO 2013/004979 A1*
33. Zhang M, Hui Q, Lou XJ, Redfern SAT, Salje EKH, Tarantino SC (2006) Dehydroxylation, proton migration, and structural changes in heated talc: an infrared spectroscopic study. *Am Miner* 91:816–825. <https://doi.org/10.2138/am.2006.1945>
34. Martin F, Micoud P, Delmotte L, Marichal CL, Dred RD, Parseval P, Mari A, Fortune JP, Salvi S, Beziat D, Ferret OG (1999) The structural formula of talc from the Trimouns deposit, Pyrenees, France. *J Can Miner* 37:997
35. Ray SS, Okamoto M (2003) Polymer/layered silicate nanocomposites: a review from preparation to processing. *Prog Polym Sci* 28:1539–1641
36. Paul DR, Robeson LM (2008) Polymer nanotechnology: nanocomposites. *Polymer* 49:3187–3204
37. Hajjalizadeh S, Barikani M, Bellah SM (2017) Synthesis and characterization of multiwall carbon nanotube/waterborne polyurethane nanocomposites. *Polym Int* 66:1074–1083. <https://doi.org/10.1002/pi.5362>
38. Castillo LA, Barbosa SE, Capiati NJ (2013) Influence of talc morphology on the mechanical properties of talc filled polypropylene. *J Polym Res* 20:152. <https://doi.org/10.1007/s10965-013-0152-2>
39. Han W (2013) Synthesis and properties of networking waterborne polyurethane/silica nanocomposites by addition of poly(ester amine) dendrimer. *Polym Compos* 34:156. <https://doi.org/10.1002/pc.22388>
40. Dumas A, Martin F, Le Roux C et al (2013) Phyllosilicates synthesis: a way of accessing edges contributions in NMR and FTIR spectroscopies. Example of synthetic talc. *Phys Chem Miner* 40:361. <https://doi.org/10.1007/s00269-013-0577-5>
41. Romo-Uribe A, Santiago-Santiago K, Zavala-Padilla G, Reyes-Mayer A, Calixto-Rodriguez M, Arcos-Casarrubias JA, Baghdachi J (2016) Waterborne layered silicate/acrylate nanocomposites by in situ emulsion polymerization: thermal and mechanical reinforcement. *Prog Org Coat* 101:59–70
42. Wu Y, Du Z, Wang H, Cheng X (2016) Preparation of waterborne polyurethane nanocomposite reinforced with halloysite nanotubes for coating applications. *J Appl Polym Sci*. <https://doi.org/10.1002/app.43949>
43. Santamaria-Echart A, Ugarte L, García-Astrain C, Arbelaiz A, Corcuera MA, Eceiza A (2016) Cellulose nanocrystals reinforced environmentally-friendly waterborne polyurethane nanocomposites. *Carbohydr Polym* 151:1203–1209

Publisher's Note Springer Nature remains neutral with regard to jurisdictional claims in published maps and institutional affiliations.

Affiliations

Guilherme Dias¹ · Manoela Prado¹ · Christophe Le Roux⁴ · Mathilde Poirier⁴ · Pierre Micoud⁴ · Rosane Ligabue^{1,2} · François Martin⁴ · Sandra Einloft^{1,3} 

¹ Post-Graduation Program in Materials Engineering and Technology, Pontifical Catholic University of Rio Grande do Sul – PUCRS, Porto Alegre, Brazil

² School of Science, Pontifical Catholic University of Rio Grande do Sul – PUCRS, Porto Alegre, Brazil

³ School of Technology, Pontifical Catholic University of Rio Grande do Sul – PUCRS, Porto Alegre, Brazil

⁴ ERT Géomatériaux, GET, Université de Toulouse, CNRS, IRD, UPS, Toulouse, France